Experimental Neurology 314 (2019) 91–99

Contents lists available at ScienceDirect

Experimental Neurology

journal homepage: www.elsevier.com/locate/yexnr

Research Paper

Bioenergetic dysfunction in a zebrafish model of acute hyperammonemic decompensation

Matthias Zielonka[a,b,*], Joris Probst[a], Matthias Carl[c], Georg Friedrich Hoffmann[a], Stefan Kölker[a,1], Jürgen Günther Okun[a,1]

[a] Center for Child and Adolescent Medicine, Division for Pediatric Neurology and Metabolic Medicine, University Hospital Heidelberg, Heidelberg, Germany
[b] Heidelberg Research Center for Molecular Medicine (HRCMM), Heidelberg, Germany
[c] Center for Integrative Biology (CIBIO), Laboratory of Translational Neurogenetics, University of Trento, Trento, Italy

ARTICLE INFO

Keywords:
Urea cycle disorders
Hyperammonemia
Bioenergetic impairment
Neurotoxicity
Zebrafish

ABSTRACT

Acute hyperammonemic encephalopathy is a life-threatening manifestation of individuals with urea cycle disorders, which is associated with high mortality rates and severe neurological sequelae in survivors. Cerebral bioenergetic failure has been proposed as one of the key mechanisms underlying hyperammonemia-induced brain damage, but data supporting this hypothesis remain inconclusive and partially contradictory. Using a previously established zebrafish model of acute hyperammonemic decompensation, we unraveled that acute hyperammonemia leads to a transamination-dependent withdrawal of 2-oxoglutarate (alpha-ketoglutarate) from the tricarboxylic acid (TCA) cycle with consecutive TCA cycle dysfunction, ultimately causing impaired oxidative phosphorylation with ATP shortage, decreased ATP/ADP-ratio and elevated lactate concentrations. Thus, our study supports and extends the hypothesis that cerebral bioenergetic dysfunction is an important pathophysiological hallmark of hyperammonemia-induced neurotoxicity.

1. Introduction

Acute hyperammonemic encephalopathy (HE) is a life-threatening manifestation of several inherited and acquired diseases characterized by an acute onset of neurological symptoms such as lethargy, seizures and coma, high mortality rates and severe neurological sequelae in survivors (Brusilow, 2002; Burgard et al., 2016). In children, hyperammonemia can originate from various acquired or inherited diseases, among which urea cycle disorders (UCDs) are a prototypic and well known disease group (Leonard and Morris, 2002; Gropman et al., 2007; Tuchman et al., 2008). UCDs are caused by inherited deficiencies of five enzymes and two transporters that are involved in the irreversible detoxification of ammonium (NH_4^+) to urea including carbamoylphosphate synthetase 1 (CPS1), ornithine transcarbamylase (OTC), argininosuccinate synthetase (ASS1), argininosuccinate lyase (ASL), arginase 1 (ARG1), citrin or aspartate/glutamate carrier and the mitochondrial ornithine transporter 1 (Haberle et al., 2012). Moreover, carbonic anhydrase VA and *N*-acetylglutamate synthetase (NAGS) are required to form bicarbonate and *N*-acetylglutamate for the formation of carbamoylphosphate, the first enzymatic step of ureagenesis. Inherited deficiencies of those two cofactor-generating enzymes are also known causes for hyperammonemic decompensation (Haberle et al., 2012; van Karnebeek et al., 2014). Cumulative incidence of UCDs is estimated between 1:35,000 to 1:50,000 newborns (Summar et al., 2013; Nettesheim et al., 2017). In individuals with UCDs, HE mainly manifests during the first days of life, but may appear at any time thereafter (Bachmann, 2003; Enns et al., 2007; Summar et al., 2008; Ah Mew et al., 2013; Kolker et al., 2015; Nettesheim et al., 2017). Mortality rates in early onset UCDs were shown to be between one third to one half of affected neonates (Bachmann, 2003; Haberle et al., 2012; Nettesheim et al., 2017), which – despite all diagnostic and therapeutic efforts during the last three decades – could not be relevantly improved

Abbreviations: ARG1, arginase 1; ASL, argininosuccinate lyase; ASS1, argininosuccinate synthetase 1; ADP, adenosine diphosphate; ATP, adenosine triphosphate; BCAA, branched-chain amino acid; CNS, central nervous system; CPS1, carbamoylphosphate synthetase 1; dpf, days post fertilization; h, hours; HE, hyperammonemic encephalopathy; hpf, hours post fertilization; M, mole; min, minutes; mM, millimole; μM, micromole; NaAc, sodium acetate; NAGS, *N*-acetylglutamate synthase; NH_4Ac, ammonium acetate; NMDA, *N*-methyl-D-aspartate; OTC, ornithine transcarbamylase; *s*, seconds; TCA, tricarboxylic acid; UCD, urea cycle disorder

* Corresponding author at: Center for Child and Adolescent Medicine, Division for Pediatric Neurology and Metabolic Medicine, University Hospital Heidelberg, Im Neuenheimer Feld 430, Heidelberg 69120, Germany.
E-mail address: matthias.zielonka@med.uni-heidelberg.de (M. Zielonka).
[1] Both authors contributed equally.

https://doi.org/10.1016/j.expneurol.2019.01.008
Received 19 September 2018; Received in revised form 18 December 2018; Accepted 12 January 2019
Available online 14 January 2019
0014-4886/

(Burgard et al., 2016), highlighting the urgent need for a better understanding of the pathophysiology underlying hyperammonemia-induced neurotoxicity and targeted therapies. Recently, it has been shown that ammoniotelic zebrafish, an organism physiologically lacking the urea cycle after hatching during early embryonic development, is a suitable model to study the diverse mechanisms of NH_4^+-induced neurotoxicity (Zielonka et al., 2018). Besides glutamine-mediated brain edema and hyperglutamatergic excitotoxicity, cerebral energy depletion has been proposed as important pathophysiological process in acute HE (Ott and Vilstrup, 2014; Natesan et al., 2016). In particular, it has been proposed that hyperammonemia inhibits the enzyme alpha-ketoglutarate dehydrogenase, which leads to an enhanced formation of glutamate and consecutively glutamine from alpha-ketoglutarate, ultimately causing TCA cycle dysfunction and ATP depletion in mitochondria (Ott et al., 2005). However, data derived from clinical investigations as well as cell-based or animal studies still remain inconclusive and partially contradictory (Ott and Vilstrup, 2014).

Therefore, we systematically studied the impact of elevated NH_4^+ concentrations on bioenergetic functions in a recently described zebrafish model of acute hyperammonemic decompensation.

2. Materials and methods

2.1. Study approval

All experiments complied with local and international regulations and ethics guidelines and were approved by the local research ethics committee (Germany, Regierungspräsidium Karlsruhe, permit AZ 35-9185.81/G-85/16). The research project was conducted according to ARRIVE guidelines (Kilkenny et al., 2010).

2.2. Zebrafish maintenance

Zebrafish (wildtype AB/AB strain) from a closed stock at the University Heidelberg were kept as previously described (Zielonka et al., 2018). Embryos were collected by natural spawning and raised in E3 medium at 28.5 °C. Developmental stages were determined according to Kimmel et al. (Kimmel et al., 1995).

2.3. Model of acute HE

The induction of acute hyperammonemic decompensation in zebrafish larvae was conducted as previously described (Zielonka et al., 2018). To investigate the effect of acute hyperammonemia on bioenergetic parameters, larvae at developmental stage 4 days post fertilization (dpf) were exposed to ammonia by addition of ammonium acetate (NH_4Ac) to the E3 medium to a final concentration of 10 mM (pH of the medium 7.3) as determined by previous survival analysis for 6 or 12 h (h), respectively, homogenized and subjected to different biochemical analyses. To control for potential non-specific effects of the acetate-compound, zebrafish larvae were exposed to sodium acetate using the same concentration, hereafter referred to as negative control (neg. ctrl.) or control cohort.

2.4. Preparation of whole larvae homogenates

Control or NH_4Ac-exposed zebrafish larvae at 4 dpf were washed 3 times with ice-cold phosphate-buffered saline (PBS) followed by manual disruption in a 1.5 ml Eppendorf tube and additional sonification. Lysates were centrifuged at 13,000 × *g* at 4 °C for 10 min. The supernatant (final volume 50 or 100 µl, depending on the subsequent analyses) was either subjected to downstream applications (e.g. biochemical analyses) or stored at −80 °C until use. Protein concentrations were quantitatively determined according to a modified Lowry protocol (Lowry et al., 1951; Helenius and Simons, 1972) using bovine serum albumin as a standard.

2.5. qRT-PCR

RNA from larvae at 4 dpf was obtained by standard procedure with TRIzol Reagent (Invitrogen). Equal amounts of RNA from each sample (500 to 800 ng) were used for cDNA synthesis applying the Maxima first strand cDNA synthesis kit (Thermo Fisher Scientific). PCR was performed on a CFX ConnectTM 180 Real-Time cycler (Biorad) (denaturation step: 95 °C for 25 s, annealing and elongation step: 60 °C for 30 s) using SensiFast SYBR™ Hi-ROX mix (Bioline) following the manufacturer's instructions. The genes of interest were amplified with the following primers:

GPT
GPT-forward: 5′-GGCATAGCGTCAGTGTCCTT-3′
GPT-reverse: 3′-AACTGCTCCTGTAGGGTTGC-5′
GPT2
GPT2-forward: 5′-CTTGGAGGAGGGTGGAACAAA-3′
GPT2-reverse: 3′-ATCCTCTGGGAAACTAGGGCT-5′
PCCA
PCCA-forward: 5′-GTGTTGGTCCTGCTCCTACC-3′
PCCA-reverse: 3′-CCTCAGCCGCCAATCTTTTG-5′
PCCB
PCCB-forward: 5′-GAAAGCAGAACCAAGCGGAG-3′
PCCB-reverse: 3′-CTCTAAAGCAGGGGTTGGTCT-5′

The expression level of elongation factor 1-α was used for normalization.

2.6. Amino acid analysis

Quantitative measurement of amino acids in larvae homogenates at 4 dpf was performed in the physiologic mode of an automatic amino acid analyzer (Biochrom 30+; Biochrom Ltd. UK) according to a slightly modified protocol of Slocum and Cummings (Slocum and Cummings, 1991). In brief, 100 µl of larvae homogenates were diluted with 100 µl of NaCl and 50 µl of sulfosalicylic acid (20%) with 2 internal standards added to the mixture. After centrifugation for 5 min at 18620 rcf (RCF, relative centrifugal force measured in force × gravity or *g*-force), the supernatant was diluted 1:2 with lithium loading buffer (Onken, Gründau, Germany). Ion exchange chromatography was used to separate amino acids by increasing pH, ion strength, and temperature of the elution buffers (Onken, Gründau, Germany). After post-column derivatization with ninhydrin, amino acids were detected at 440 nm and 570 nm. For data collection and processing, ChromStar (SCPA,-Weyme-Leeste, Germany) was used. The system was calibrated before each batch and quality controls were measured to check system stability and reliability. For each sample, detected amino acids were normalized to the internal standards. Thereafter, amino acid content was normalized to the corresponding protein concentration in each sample.

2.7. Quantification of 2-oxoglutarate (alpha-ketoglutarate)

Alpha-ketoglutarate was determined in whole larvae homogenates of control or NH_4Ac-exposed larvae at 4 dpf using a colorimetric alpha-ketoglutarate assay kit (Abcam) following the manufacturer's instructions. In this assay, alpha-ketoglutarate is converted to ultimately form pyruvate, which then is utilized to convert the optical density of a nearly colorless probe. The generated colorimetric signal within the reaction is proportional to the alpha-ketoglutarate concentration. Briefly, after washing with ice-cold PBS, larvae were homogenized in alpha-ketoglutarate assay buffer and centrifuged at 13,000 × *g* at 4 °C for 10 min in an Eppendorf centrifuge to remove insoluble material. The supernatant was transferred to a new Eppendorf tube and deproteinized using perchloric acid in a final concentration of 1 M. Following centrifugation at 13,000 × *g* at 4 °C for 15 min, the supernatant was added to an alpha-ketoglutarate converting enzyme mix and incubated at

37 °C in the dark for 30 min. Hereafter, the optical density was determined at 570 nm using a SpectraMax Plus 384 microplate reader (Molecular Devices). Each sample was additionally subjected to colorimetric readout in the absence of alpha-ketoglutarate. Sample background values were subtracted from sample readings for correction. Alpha-ketoglutarate concentrations were determined by extrapolation from a standard curve. Measurements were performed in duplicates for each experimental series. Alpha-ketoglutarate concentrations were normalized to the protein content in the respective samples.

2.8. Quantification of pyruvate and lactate

For quantification of pyruvate and lactate, homogenates of control or NH_4Ac-exposed larvae at 4 dpf were subjected to a colorimetric lactate dyhydrogenase enzyme assay. Briefly, pyruvate content was analyzed by addition of lactate dehydrogenase and NADH to the homogenate exploiting the lactate dehydrogenase reaction, which results in the formation of lactate and NAD^+. Pyruvate concentrations were quantitatively determined by the reduction of NADH concentrations at a wavelength of 340 nm using an Olympus AU 400 chemistry analyzer. Analogously, lactate concentrations were quantified by applying the lactate dehydrogenase reaction in reverse and subsequently measuring the increase of NADH concentrations at the same wavelength. Pyruvate and lactate concentrations were normalized to the protein content in each sample.

2.9. Quantitative analysis of TCA cycle metabolites

TCA cycle metabolites were determined in larvae homogenates at 4 dpf according to Hoffmann et al. (Hoffmann et al., 1989) and Sweetman (Sweetman, 1991). In brief, larvae homogenates equivalent to 700 µg total protein (range 600 to 800 µg total protein) were acidified with hydrochloric acid and extracted twice with ethylacetate. After removal of the solvent the residue was derivatized with *N*-methyl-*N*-trimethylsilyl-heptafluorbutyramide (MSHFBA, Macherey-Nagel, Düren, Germany). The resulting trimethylsilyl derivatives were analyzed on the single quadrupole mass spectrometer DSQ II (Thermo Fisher Scientific GmbH) coupled to the gaschromatograph TRACE GC (Thermo Fisher Scientific GmbH). The mass spectrometer was run in full scan mode (*m/z* 50 to *m/z* 650) with electron impact ionization. Gas chromatographic separation was achieved on a capillary column (DB-5MS, 30 m × 0.25 mm; film thickness: 0.25; J&W Scientific, Folsom, CA, USA) using helium as a carrier gas. A volume of 1 µl of the derivatized sample was injected in splitless mode. GC temperature parameters were 80 °C for 2 min, ramp 50 °C/min to 150 °C, ramp 10 °C/min to 300 °C. Injector temperature was set to 260 °C and interface temperature to 260 °C. TCA cycle intermediates were normalized to the total protein content and are presented as µmol per g protein.

2.10. Quantitative analysis of C2-carnitine

C2-carnitine was determined in larvae homogenates at 4 dpf by electrospray ionization tandem mass spectrometry (ESI-MS/MS) according to a modified method as previously described (Sauer et al., 2015) using a Quattro Ultima triple quadrupole mass spectrometer (Micromass, Manchester, UK) equipped with an electrospray ion source and a Micromass MassLynx data system. In brief, 5 µl larvae homogenates were given on a 4.7 mm filter paper punch, dried at room temperature overnight and extracted with 100 µl of deuterium labelled standard solution in methanol. After 20 min, the samples were centrifuged and the extract was evaporated to dryness, reconstituted in 60 µl of 3 N HCl/butanol, placed in sealed microtiter plates, and incubated at 65 °C for 15 min. The resulting mixtures were dried, and each residue was finally reconstituted in 100 µl solvent of acetonitrile/water/formic acid (50: 50: 0.025 *v*/v/v) prior measurement. C2-carnitine levels were normalized to the protein concentration in the respective samples.

2.11. Quantitative analysis of intracellular glucose concentrations

Intracellular glucose concentrations were determined in deproteinized whole body lysates using the AmplexTM Red Glucose/Glucose Oxidase Assay Kit (Invitrogen) according to the manufacturer's instructions. Glucose concentrations were normalized to the total protein content in each sample.

2.12. Quantitative analysis of ATP and ADP levels

Concentrations of ATP and ADP in larvae homogenates at 4 dpf were quantitatively determined using commercially available colorimetric ATP and ADP assay kits (Sigma-Aldrich) following the manufacturer's instructions. ATP and ADP levels were normalized to the protein content in the respective samples. ATP/ADP-ratios were calculated by dividing the normalized ATP concentrations by the corresponding normalized ADP values of each sample.

2.13. Statistical analysis

Data are expressed as mean +/− SD unless otherwise stated. Values for individual measurements are illustrated within scatterplots. All experimental procedures were performed five times in biological replicates ($n = 5$ with 50 larvae per group and experiment). Differences between mean values of groups were evaluated by two-tailed Student's *t*-test using the Prism software (GraphPad Software, La Jolla, CA, USA). P values < 0.05 were considered significant.

3. Results

3.1. Acute hyperammonemia causes transamination-dependent withdrawal of alpha-ketoglutarate from the TCA cycle

Transamination processes involving activity of ornithine aminotransferase (OAT) have been shown to cause hyperglutamatergic excitotoxicity by transferring the amino group from ornithine onto alpha-ketoglutarate to ultimately form glutamate under hyperammonemic conditions (Zielonka et al., 2018). To test whether withdrawal of alpha-ketoglutarate from the TCA cycle might contribute to cerebral energy depletion in acute hyperammonemia, we have quantified alpha-ketoglutarate concentrations in whole body lysates of zebrafish larvae at 4 dpf upon exposure to 10 mM NH_4Ac. Acute hyperammonemia caused a significant reduction of alpha-ketoglutarate levels in NH_4Ac-exposed larvae 6 h after start of exposure when compared to the negative control cohort (Fig. 1a). This effect was even more pronounced 12 h after start of NH_4Ac-exposure. In parallel, glutamate concentrations increased in the presence of 10 mM NH_4Ac with concomitantly decreased alanine concentrations (Fig. 1b, c). Since alanine aminotransferases reversibly catalyze the amidation of alpha-ketoglutarate by transfer of an amino group from alanine to alpha-ketoglutarate to form glutamate and pyruvate (Benuck and Lajtha, 1975), we hypothesized that activity of alanine aminotransferases are functionally relevant for the observed changes. In zebrafish, two homologs of alanine aminotransferases, GPT and GPT2, have been described (Steinke et al., 2006; Mirando et al., 2015). Since gene induction of ammonium-metabolizing enzymes such as glutamine synthetases and glutaminases have been reported to occur as adaptive response to elevated NH_4^+ concentrations (Zielonka et al., 2018), we analyzed the regulation of gene expression of alanine aminotransferases under hyperammonemic conditions. Whereas mRNA expression of GPT was unaltered in zebrafish larvae exposed to NH_4Ac at 4 dpf (Fig. 1d), GPT2 expression significantly increased after 12 h of NH_4Ac exposure (Fig. 1e), confirming that gene induction occurs on the level of alanine aminotransferase GPT2.

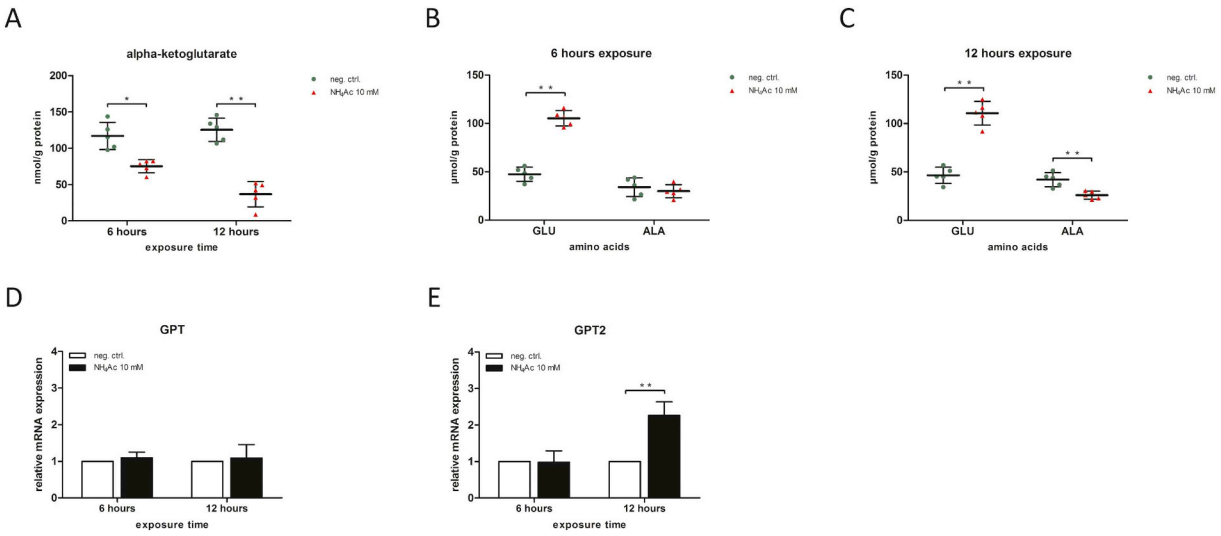

Fig. 1. Acute hyperammonemia is associated with increased glutamate concentrations and concomitant depletion of alanine and alpha-ketoglutarate.
Zebrafish larvae at 4 dpf were exposed to 10 mM NH_4Ac for 6 or 12 h, respectively and subjected to quantitative analysis of alpha-ketoglutarate levels as described under *Materials and Methods*, amino acids using HPLC or mRNA expression analysis of GPT and GPT2 applying qRT-PCR. Exposed larvae exhibited a significant depletion of alpha-ketoglutarate levels after 6 h, with a further decline after 12 h of exposure (A). Simultaneously, NH_4^+-exposure caused increased glutamate concentrations after 6 and 12 h with concomitantly decreased concentrations of alanine when compared to the control cohort (B, C). Intriguingly, exposure to 10 mM NH_4Ac induced mRNA expression of GPT2 (E), but not of alanine aminotransferase isoform GPT (D). Data are expressed as nmol per g protein (A) µmol per g protein (B, C) or fold-change (D, E) (whole body lysates, $n = 5$ with 50 larvae per group and experiment; Student's *t*-test, *P < 0.05, **P < 0.01).

3.2. TCA cycle dysfunction is a major hallmark of acute hyperammonemic decompensation

To further determine the effects of alpha-ketoglutarate withdrawal on TCA cycle function under hyperammonemic conditions, we quantitatively analyzed intermediary metabolites of the TCA cycle using gas chromatography/mass spectrometry (GC/MS). While the TCA cycle intermediates succinic, fumaric and malic acid remained unaltered after 6 h of exposure to 10 mM NH_4Ac (Fig. 2a), NH_4^+-exposed larvae exhibited significantly decreased concentrations of fumaric and malic acid after 12 h (Fig. 2b), indicating impaired TCA cycle function in acute HE. In contrast, succinic acid content was unchanged in whole body lysates in the exposed larvae when compared to the control cohort after 12 h (Fig. 2b). To further investigate effects of acute hyperammonemia on TCA cycle dysfunction, we quantitatively analyzed lactate, glucose, pyruvate and C2-carnitine concentrations. Lactate levels were increased in larvae exposed to 10 mM NH_4Ac after 6 and 12 h (Fig. 3a). Moreover, intracellular glucose concentrations were decreased in NH_4^+-exposed larvae as opposed to the control cohort after 6 and 12 h (Fig. 3b), suggesting enhanced anaerobic glycolysis as additional source of ATP production under hyperammonemic conditions. Intriguingly, pyruvate concentrations were simultaneously increased in the exposed larvae 6 and 12 h after start of NH_4^+-exposure with concomitantly elevated C2-carnitine levels after 12 h of exposure (Fig. 3c, d).

3.3. Anaplerosis via enhanced propionate oxidation leads to decreased BCAA concentrations in acute hyperammonemic decompensation

Since anaplerotic reactions have been proposed to compensate for TCA cycle dysfunction by supplementation of carbon backbones under hyperammonemic conditions, we further investigated whether propionate oxidation is enhanced in the NH_4^+-exposed zebrafish cohort. Intriguingly, expression of both subunits of propionyl-CoA carboxylase (PCC), PCC subunit alpha (PCCA) and PCC subunit beta (PCCB) is induced already after 6 h of exposure to 10 mM NH_4Ac (Fig. 4a, b), with a further increased expression of PCCB after 12 h of NH_4^+-exposure. Whereas concentrations of branched-chain amino acids (BCAAs) valine, leucine and isoleucine remained unaltered after 6 h of exposure to 10 mM NH_4Ac (Fig. 4c), exposed larvae displayed decreased concentrations of all three BCAAs after 12 h (Fig. 4d), indicating enhanced

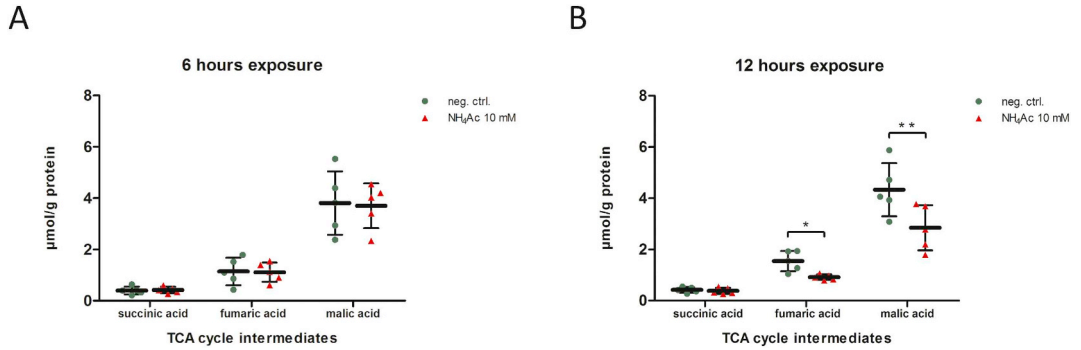

Fig. 2. The TCA cycle is dysfunctional under hyperammonemic conditions. Zebrafish larvae at 4 were subjected to 10 mM NH_4Ac for 6 (A) or 12 h (B), followed by quantification of TCA cycle metabolites applying GC/MS. While concentrations of succinic, fumaric and malic acid remained unchanged 6 h after start of NH_4^+-exposure (A), acute hyperammonemia induced a significant depletion of fumaric and malic acid after 12 h (B). In contrast, succinic acid levels were not altered in the exposed larvae after 12 h when compared to the control cohort (B). Data are expressed as µmol per g protein (whole body lysates, $n = 5$ with 50 larvae per group and experiment; Student's t-test, *P < 0.05, **P < 0.01).

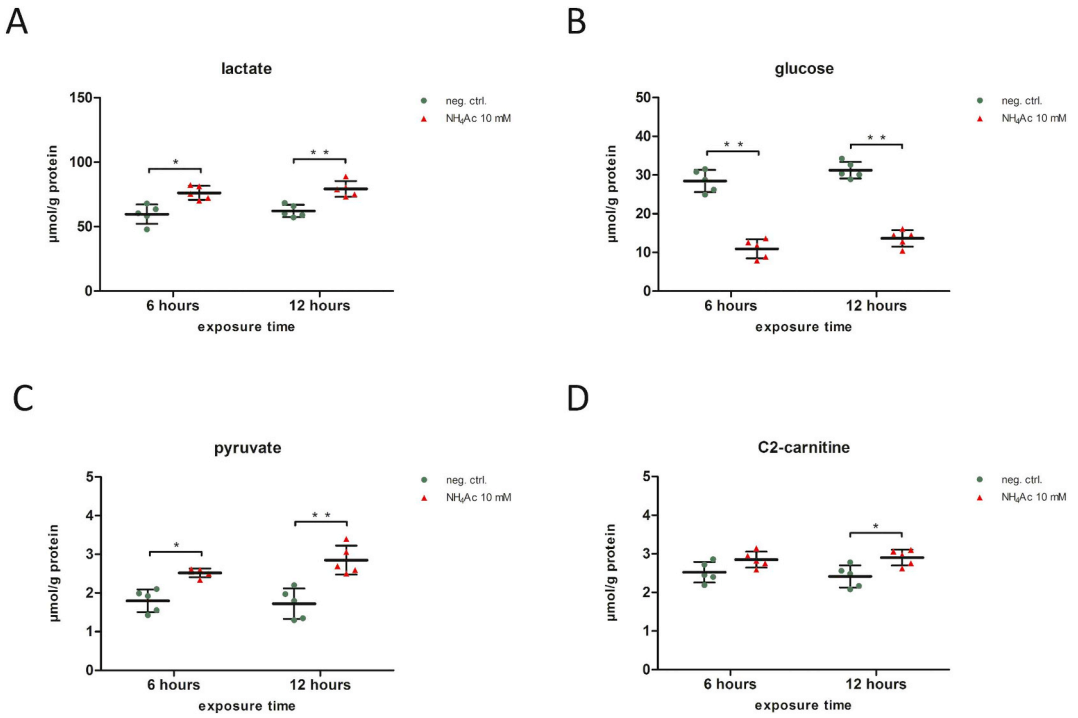

Fig. 3. Lactate, pyruvate and C2-carnitine concentrations are elevated with concomitantly decreased intracellular glucose levels in acute HE. Zebrafish larvae at 4 dpf were exposed to 10 mM NH_4Ac for 6 or 12 h, respectively. Lactate (A) and pyruvate (C) concentrations were quantitatively analyzed in homogenates of control and exposed larvae applying the lactate dyhydrogenase reaction as described under *Materials and methods*. Intracellular glucose concentrations (B) were quantitatively analyzed using a commercially available kit as outline under *Materials and methods*. C2-carnitine levels (D) were determined by ESI-MS/MS. Larvae exposed to 10 mM NH_4Ac exhibited significantly elevated lactate concentrations (A) with concomitantly decreased intracellular glucose concentrations (B) after 6 and 12 h. While pyruvate concentrations were elevated in the NH_4^+-exposed larvae after 6 and 12 h (C), exposed larvae exhibited simultaneously increased levels of C2-carnitine 12 h after start of exposure (D). Data are expressed as µmol per g protein (whole body lysates, $n = 5$ with 50 larvae per group and experiment, Student's t-test, *$P < 0.05$, **$P < 0.01$).

anaplerosis by increased propionate oxidation for the formation of succinyl-CoA, which supplies the TCA cycle with succinic acid in acute hyperammonemic conditions.

3.4. Acute HE is associated with ATP shortage and decreased ATP/ADP-ratio

Under normal conditions the TCA cycle generates NADH and $FADH_2$ as electron donors for ATP production via oxidative phosphorylation. Hence, our observation of impaired TCA cycle function led to the assumption, that acute hyperammonemia might compromise oxidative phosphorylation ultimately resulting in ATP shortage. Therefore, we investigated the effect of elevated NH_4^+-concentrations on ATP and ADP levels. As hypothesized, exposed larvae demonstrated significantly reduced concentrations of ATP with simultaneously increased levels of ADP (Fig. 5a, b), leading to significantly decreased ATP/ADP-ratio documenting severe bioenergetic depletion after 12 h of NH_4^+ exposure when compared to the negative control cohort (Fig. 5c).

4. Discussion

Acute hyperammonemia has been suggested to result in cerebral energy impairment leading to brain damage, but clinical and experimental data were inconclusive and partially contradictory (Ott and Vilstrup, 2014).

Here, we address this question through bioenergetic analysis in a recently established zebrafish model for acute hyperammonemic decompensation *in vivo*. Using this standardized NH_4^+-exposure model, it is shown that acute hyperammonemia leads to a transamination-dependent withdrawal of alpha-ketoglutarate from the TCA cycle, with consecutively impaired TCA cycle function as indicated by decreased fumaric and malic acid concentrations, ultimately resulting in impaired oxidative phosphorylation with ATP shortage, decreased ATP/ADP-ratio and elevated lactate concentrations.

The pathophysiological basis of hyperammonemia-induced neurotoxicity is complex and was shown to be caused by alterations in various metabolic pathways including cerebral energy metabolism due to elevated NH_4^+ concentrations. Mice deficient for the urea cycle enzyme OTC show decreased creatine and ATP content in the brain as sign of cerebral energy depletion (Ratnakumari et al., 1992; Ratnakumari et al., 1996). Accordingly, cultured primary rat astrocytes exposed to NH_4^+ develop mitochondrial permeability transition, which ultimately results in the production of reactive oxygen species and impaired ATP generation leading to cell death (Bai et al., 2001; Alvarez et al., 2011). Cataplerotic removal of alpha-ketoglutarate from the TCA cycle due to enhanced glutamate synthesis has been proposed as major contributing factor to the observed bioenergetic changes under hyperammonemic conditions (Bessman and Bessman, 1955). In the investigated *in vivo* model of acute hyperammonemic decompensation, acute hyperammonemia caused a time-dependent strong depletion of alpha-ketoglutarate levels with concomitantly elevated glutamate concentrations and decreased alanine content, suggesting enhanced transamination processes exerted by alanine aminotransferases as source of the cataplerotic withdrawal of alpha-ketoglutarate. Consistently, mRNA expression levels of GPT2, but not GPT were increased in the exposed larvae as judged by qRT-PCR analysis in response to elevated NH_4^+. Gene induction of NH_4^+-metabolizing enzymes was recently demonstrated in acute hyperammonemia (Zielonka et al., 2018). Strikingly, human GPT2 is expressed in various tissues with high expression levels in the brain (Yang et al., 2002). Since it was shown in extracted cerebral rat mitochondria that NH_4^+ at a concentration range between 0.2 and 2.0 mM inhibited alpha-ketoglutarate dehydrogenase

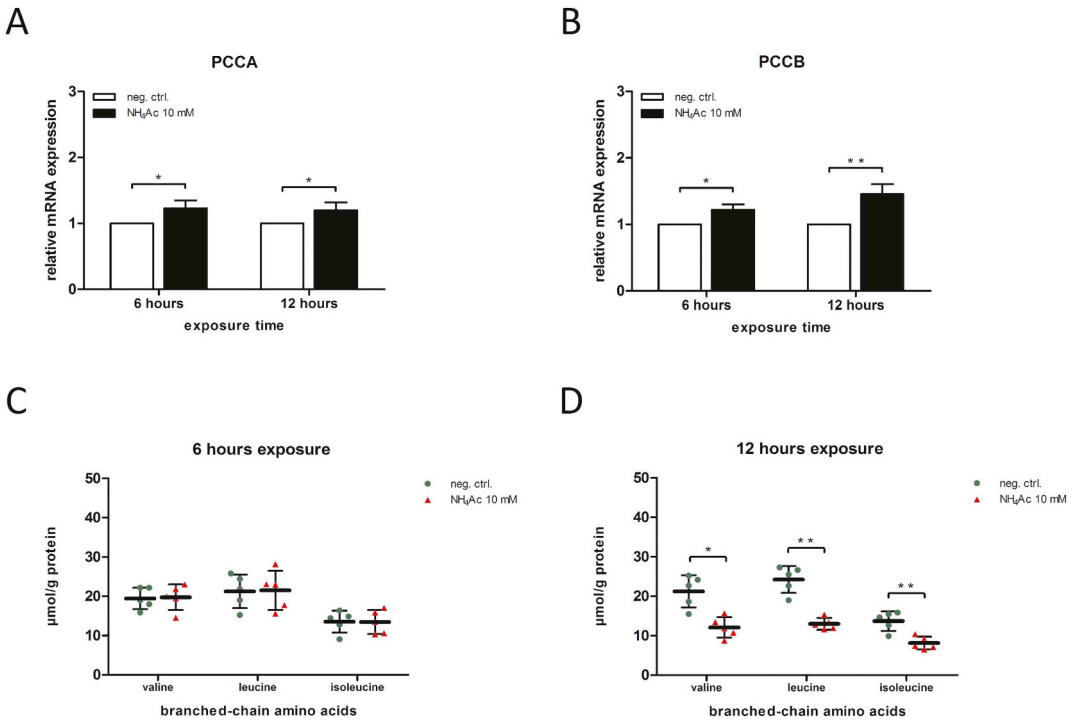

Fig. 4. Anaplerosis via increased propionate oxidation leads to decreased BCAA concentrations in hyperammonemic decompensation.
Zebrafish larvae at 4 dpf were subjected to 10 mM NH_4Ac for 6 and 12 h, respectively, followed by mRNA expression analysis of PCCA and PCCB applying qRT-PCR (A, B) or quantification of BCAA concentrations using HPLC (C, D). Exposure to NH_4^+ induced expression of both PCC-subunits, PCCA (A) and PCCB (B) after 6 and 12 h, implicating increased propionate oxidation under hyperammonemic conditions. While intracellular concentrations of BCAAs remained unaltered in the NH_4^+-exposed cohort after 6 h (C), exposed larvae exhibited decreased valine, leucine and isoleucine levels after 12 h (D). Data are expressed as fold-change (A, B) or µmol per g protein (C, D) (whole body lysates, $n = 5$ with 50 larvae per group and experiment, Student's t-test, *P < 0.05, **P < 0.01).

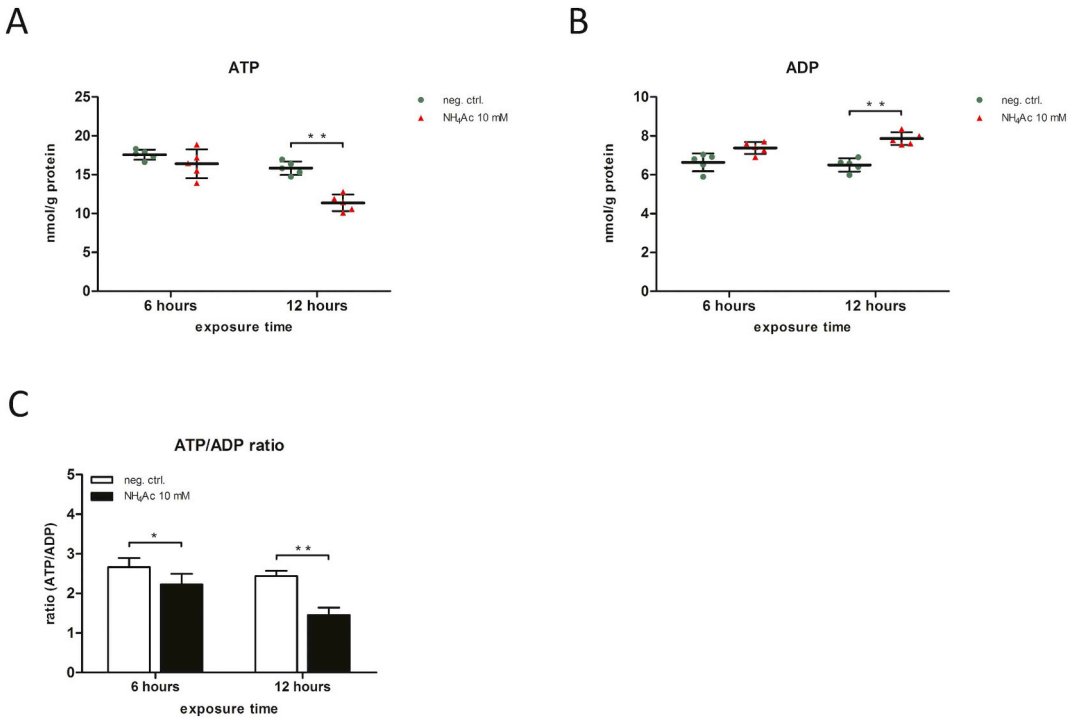

Fig. 5. Bioenergetic depletion indicated by decreased ATP-levels and ATP/ADP-ratio is a major hallmark of acute HE. Zebrafish larvae were exposed to NH_4Ac in a final concentration of 10 mM for 6 and 12 h. ATP (A) and ADP (B) concentrations in the respective larvae homogenates were quantitatively analyzed using colorimetric assay kits. ATP/ADP-ratio (C) was calculated by dividing the ATP concentrations by the corresponding ADP values. NH_4^+-exposed larvae showed significantly decreased ATP-levels (A) with concomitantly increased ADP concentrations (B) after 12 h of exposure to NH_4Ac, resulting in a strong decrease of ATP/ADP-ratio when compared to the control cohort (C). Data are expressed as nmol per g protein (A, B) or relative ATP/ADP-ratio (C) (whole body lysates, $n = 5$ with 50 larvae per group and experiment, Student's t-test, *P < 0.05, **P < 0.01).

(Lai and Cooper, 1986, 1991), the block in TCA cycle flux at the level of alpha-ketoglutarate is likely to enhance transamination and therewith results in increased consumption of alpha-ketoglutarate for the formation of glutamate by GPT2.

Intriguingly, acute hyperammonemia not only caused depletion of alpha-ketoglutarate, but also led to a general dysfunction of the TCA cycle as indicated by decreased concentrations of the TCA cycle intermediates fumaric and malic acid in the exposed cohort. This observation was recently corroborated in cultured human primary hepatocytes, which exhibited significantly decreased levels of alpha-ketoglutarate, malate and citrate along with increased glutamine concentrations upon exposure to 10 mM ammonium chloride (Wang et al., 2014), clearly supporting our findings. Synergistically to the withdrawal of alpha-ketoglutarate, impaired TCA cycle function during hyperammonemia is also caused by direct NH_4^+-induced inhibition of further TCA cycle enzymes including pyruvate dehydrogenase complex and isocitrate dehydrogenase (Katunuma et al., 1966; Zwingmann et al., 2003). In contrast to fumaric and malic acid, concentrations of succinic acid remained unchanged in zebrafish larvae under hyperammonemic conditions. Moreover, mRNA expression of both PCC subunits, PCCA and PCCB, was increased already after 6 h of exposure to 10 mM NH_4Ac, while initially unchanged BCAA concentrations were significantly decreased 12 h after start of exposure. These findings indicate that propionate oxidation as major anaplerotic mechanism during hyperammonemia is enhanced and supplies comprised TCA cycle function with carbon backbones. Enhanced anaplerosis as compensatory mechanisms in hyperammonemia has been described before (Kanamatsu and Tsukada, 1999; Shen et al., 1999; Sibson et al., 2001; Zwingmann et al., 2003), highlighting the role of the deamination of BCAAs for the generation of succinyl-CoA (isoleucine, valine), which can supply the TCA cycle with important carbon backbones. Consistently, patients suffering from advanced liver disease exhibit decreased BCAA levels in plasma (Muting and Wortmann, 1956) and isoleucine and leucine have been shown to be the only amino acids with significant cerebral uptake from the blood in patients with fulminant hepatic failure (Strauss et al., 2001). Moreover, hyperammonemia stimulated cerebral BCAA transaminases, thereby enhancing the use of isoleucine and valine for anaplerotic reactions as well as transamination to generate glutamate and glutamine (valin, leucine and isoleucine) via activities of BCAT1 and BCAT2, respectively (Jessy et al., 1990; Tonjes et al., 2013). However, the compensatory effect of increased propionate oxidation seems to decrease over time and becomes insufficient to maintain residual TCA cycle activity, as indicated by the high consumption of BCAAs 12 h after start of NH_4^+-exposure. In the present study, we identified elevated pyruvate, C2-carnitine and lactate concentrations, further supporting the notion of TCA cycle dysfunction in acute HE. While direct NH_4^+-induced inhibition of pyruvate dehydrogenase complex most likely contributes to the observed biochemical changes, increased lactate concentrations in the NH_4^+-exposed larvae might also indicate that ATP is generated to a higher extent via anaerobic glycolysis, which is further supported by the finding of decreased intracellular glucose concentrations in the NH_4^+-exposed larvae in our study. Moreover, increased blood and brain lactate levels as marker for impaired oxidative phosphorylation have been documented in patients with hepatic encephalopathy and end-stage fulminant hepatic failure (Wendon et al., 1994; Walsh et al., 1999). Extracellular elevation of lactate was also reported in a cohort of patients with acute liver failure (Tofteng et al., 2002). Increased lactate concentrations have also been observed in a rat model of acute liver failure as well as in primary astrocytes exposed to NH_4^+ (Zwingmann et al., 2003).

In this study, zebrafish larvae exposed to 10 mM NH_4Ac ultimately exhibited ATP shortage with significantly decreased ATP/ADP-ratio, suggesting cerebral energy depletion as a relevant pathophysiological factor in acute HE. Decreased cerebral ATP concentrations have been described in brains of portocaval-shunted rats infused with NH_4^+ (Hindfelt et al., 1977), in a rat model of chronic HE (Astore and Boicelli, 2000), as well as in mice deficient for the urea cycle enzyme OTC (Rao et al., 1997). Finally, cultured primary astrocytes exhibited decreased ATP concentrations when treated with ammonium chloride (Haghighat et al., 2000). Of note, ATP shortage is present only 12 h after start of NH_4^+-exposure. In light of the biochemical data, it is tempting to speculate that increased glycolysis along with enhanced propionate oxidation are initially compensating the effect of alpha-ketoglutarate depletion to maintain residual TCA cycle function and ATP generation, but are successively becoming insufficient to prevent bioenergetic failure as hyperammonemia persists. Besides interference with TCA cycle function, ATP shortage might also be caused by excessive hyperglutamatergic activation of NMDA receptors in acute hyperammonemia which increases the activity of Na^+-K^+-ATPase, causing enhanced consumption of ATP (Kosenko et al., 1994; Marcaida et al., 1996). Hyperglutamatergic and hyperglutaminergic hyperammonemia with consecutive excessive activation of NMDA receptors was shown to be relevant for the pathophysiology of acute HE in a previous study (Zielonka et al., 2018).

Given that TCA cycle dysfunction with drain of alpha-ketoglutarate is a major hallmark of hyperammonemia-induced brain damage, it is tempting to assume that supplementation of alpha-ketoglutarate or other TCA cycle intermediates might prove beneficial in acute hyperammonemic decompensation for individuals with UCDs. Intriguingly, administration of alpha-ketoglutarate was shown to significantly reduce hyperammonemia along with plasma levels of pyruvate and lactate in cirrhotic patients (Salerno et al., 1983) and improved hyperammonemia-induced biochemical changes in rats exposed to NH_4Ac (Velvizhi et al., 2002). Moreover, supplementation with BCAAs to enhance anaplerosis and therewith improve TCA cycle function might be another therapeutic strategy to correct bioenergetic failure in acute hyperammonemia. Of note, oral supplementation with BCAAs improved survival in a rat model of liver cirrhosis (Kajiwara et al., 1998). In addition, supplementation with essential amino acids and BCAAs is recommended by a recent Cochrane study for individuals with hepatic encephalopathy (Gluud et al., 2017) as well as suggested guidelines for individuals with UCDs, in particular if natural protein intake is very low (Haberle et al., 2012).

5. Conclusions

Significant cerebral energy impairment caused by transamination-dependent withdrawal of alpha-ketoglutarate from the TCA cycle with consecutively impaired TCA cycle function is an important mechanism in acute hyperammonemic decompensation, ultimately causing ATP shortage and decreased ATP/ADP-ratio. Since zebrafish have already been used to systematically test new therapeutic approaches in acute hyperammonemia (Zielonka et al., 2018), pharmacologically correcting bioenergetic failure in this model organism might be a successful strategy to identify new therapeutic targets or agents in the future.

Acknowledgements

We thank K. Schwarz, P. Feyh, S. Exner, F. Kratzer and S. Wächter at the Metabolic Center Heidelberg for excellent technical support and T. Fleming at the Department for Endocrinology, Metabolic Medicine and Clinical Chemistry of the University Hospital Heidelberg for perfoming intracellular glucose measurements. M. Zielonka was supported by the Physician-Scientist Program at Ruprecht-Karls-University Heidelberg, Faculty of Medicine, a Career Development Fellowship provided by the Heidelberg Research Center for Molecular Medicine (HRCMM) in the framework of Excellence Initiative II of the German Research Foundation and a Trainee Research Fellowship provided by the Urea Cycle Disorders Consortium (UCDC).

Author Contributions

MZ, SK and JGO designed the study and the experimental outline. MZ and JP performed experiments. MZ, JP, SK and JGO analyzed and interpreted the obtained data sets. MC and GFH helped in data analysis and interpretation. MZ, JGO and SK wrote the manuscript. All authors critically revised the manuscript for intellectual content and gave approval for the final version to be published.

Conflict of Interest Statement

All authors declare that there exist no potential conflicts of interest with regard to the research, authorship, and/or publication of this article.

References

Ah Mew, N., Krivitzky, L., McCarter, R., Batshaw, M., Tuchman, M., 2013. Urea cycle disorders consortium of the rare diseases clinical research N. clinical outcomes of neonatal onset proximal versus distal urea cycle disorders do not differ. J. Pediatr. 162 (2), 324–329 (e1).

Alvarez, V.M., Rama Rao, K.V., Brahmbhatt, M., Norenberg, M.D., 2011. Interaction between cytokines and ammonia in the mitochondrial permeability transition in cultured astrocytes. J. Neurosci. Res. 89 (12), 2028–2040.

Astore, D., Boicelli, C.A., 2000. Hyperammonemia and chronic hepatic encephalopathy: an in vivo PMRS study of the rat brain. MAGMA 10 (3), 160–166.

Bachmann, C., 2003. Outcome and survival of 88 patients with urea cycle disorders: a retrospective evaluation. Eur. J. Pediatr. 162 (6), 410–416.

Bai, G., Rama Rao, K.V., Murthy, C.R., Panickar, K.S., Jayakumar, A.R., Norenberg, M.D., 2001. Ammonia induces the mitochondrial permeability transition in primary cultures of rat astrocytes. J. Neurosci. Res. 66 (5), 981–991.

Benuck, M., Lajtha, A., 1975. Aminotransferase activity in brain. Int. Rev. Neurobiol. 17, 85–129.

Bessman, S.P., Bessman, A.N., 1955. The cerebral and peripheral uptake of ammonia in liver disease with an hypothesis for the mechanism of hepatic coma. J. Clin. Invest. 34 (4), 622–628.

Brusilow, S.W., 2002. Hyperammonemic encephalopathy. Medicine (Baltimore) 81 (3), 240–249.

Burgard, P., Kolker, S., Haege, G., Lindner, M., Hoffmann, G.F., 2016. Neonatal mortality and outcome at the end of the first year of life in early onset urea cycle disorders—review and meta-analysis of observational studies published over more than 35 years. J. Inherit. Metab. Dis. 39 (2), 219–229.

Enns, G.M., Berry, S.A., Berry, G.T., Rhead, W.J., Brusilow, S.W., Hamosh, A., 2007. Survival after treatment with phenylacetate and benzoate for urea-cycle disorders. N. Engl. J. Med. 356 (22), 2282–2292.

Gluud, L.L., Dam, G., Les, I., Marchesini, G., Borre, M., Aagaard, N.K., et al., 2017. Branched-chain amino acids for people with hepatic encephalopathy. Cochrane Database Syst. Rev. 5, CD001939.

Gropman, A.L., Summar, M., Leonard, J.V., 2007. Neurological implications of urea cycle disorders. J. Inherit. Metab. Dis. 30 (6), 865–879.

Haberle, J., Boddaert, N., Burlina, A., Chakrapani, A., Dixon, M., Huemer, M., et al., 2012. Suggested guidelines for the diagnosis and management of urea cycle disorders. Orphanet J. Rare Dis. 7, 32.

Haghighat, N., McCandless, D.W., Geraminegad, P., 2000. The effect of ammonium chloride on metabolism of primary neurons and neuroblastoma cells in vitro. Metab. Brain Dis. 15 (2), 151–162.

Helenius, A., Simons, K., 1972. The binding of detergents to lipophilic and hydrophilic proteins. J. Biol. Chem. 247 (11), 3656–3661.

Hindfelt, B., Plum, F., Duffy, T.E., 1977. Effect of acute ammonia intoxication on cerebral metabolism in rats with portacaval shunts. J. Clin. Invest. 59 (3), 386–396.

Hoffmann, G., Aramaki, S., Blum-Hoffmann, E., Nyhan, W.L., Sweetman, L., 1989. Quantitative analysis for organic acids in biological samples: batch isolation followed by gas chromatographic-mass spectrometric analysis. Clin. Chem. 35 (4), 587–595.

Jessy, J., Rao, V.L., Murthy, C.R., 1990. Effects of partial hepatectomy on the enzymes of cerebral glutamate and branched-chain amino acid metabolism. Biochem. Int. 20 (1), 107–115.

Kajiwara, K., Okuno, M., Kobayashi, T., Honma, N., Maki, T., Kato, M., et al., 1998. Oral supplementation with branched-chain amino acids improves survival rate of rats with carbon tetrachloride-induced liver cirrhosis. Dig. Dis. Sci. 43 (7), 1572–1579.

Kanamatsu, T., Tsukada, Y., 1999. Effects of ammonia on the anaplerotic pathway and amino acid metabolism in the brain: an ex vivo ^{13}C NMR spectroscopic study of rats after administering [2-^{13}C] glucose with or without ammonium acetate. Brain Res. 841 (1–2), 11–19.

Katunuma, N., Okada, M., Nishii, Y., 1966. Regulation of the urea cycle and TCA cycle by ammonia. Adv. Enzym. Regul. 4, 317–336.

Kilkenny, C., Browne, W., Cuthill, I.C., Emerson, M., Altman, D.G., Group NCRRGW, 2010. Animal research: reporting in vivo experiments: the ARRIVE guidelines. Br. J. Pharmacol. 160 (7), 1577–1579.

Kimmel, C.B., Ballard, W.W., Kimmel, S.R., Ullmann, B., Schilling, T.F., 1995. Stages of embryonic development of the zebrafish. Dev. Dyn. 203 (3), 253–310.

Kolker, S., Garcia-Cazorla, A., Valayannopoulos, V., Lund, A.M., Burlina, A.B., Sykut-Cegielska, J., et al., 2015. The phenotypic spectrum of organic acidurias and urea cycle disorders. Part 1: the initial presentation. J. Inherit. Metab. Dis. 38 (6), 1041–1057.

Kosenko, E., Kaminsky, Y., Grau, E., Minana, M.D., Marcaida, G., Grisolia, S., et al., 1994. Brain ATP depletion induced by acute ammonia intoxication in rats is mediated by activation of the NMDA receptor and Na+,K(+)-ATPase. J. Neurochem. 63 (6), 2172–2178.

Lai, J.C., Cooper, A.J., 1986. Brain alpha-ketoglutarate dehydrogenase complex: kinetic properties, regional distribution, and effects of inhibitors. J. Neurochem. 47 (5), 1376–1386.

Lai, J.C., Cooper, A.J., 1991. Neurotoxicity of ammonia and fatty acids: differential inhibition of mitochondrial dehydrogenases by ammonia and fatty acyl coenzyme A derivatives. Neurochem. Res. 16 (7), 795–803.

Leonard, J.V., Morris, A.A., 2002. Urea cycle disorders. Semin. Neonatol. 7 (1), 27–35.

Lowry, O.H., Rosebrough, N.J., Farr, A.L., Randall, R.J., 1951. Protein measurement with the Folin phenol reagent. J. Biol. Chem. 193 (1), 265–275.

Marcaida, G., Kosenko, E., Minana, M.D., Grisolia, S., Felipo, V., 1996. Glutamate induces a calcineurin-mediated dephosphorylation of Na+,K(+)-ATPase that results in its activation in cerebellar neurons in culture. J. Neurochem. 66 (1), 99–104.

Mirando, A.C., Fang, P., Williams, T.F., Baldor, L.C., Howe, A.K., Ebert, A.M., et al., 2015. Aminoacyl-tRNA synthetase dependent angiogenesis revealed by a bioengineered macrolide inhibitor. Sci. Rep. 5, 13160.

Muting, D., Wortmann, V., 1956. Amino acid metabolism in liver diseases. Dtsch. Med. Wochenschr. 81 (46), 1853–1856.

Natesan, V., Mani, R., Arumugam, R., 2016. Clinical aspects of urea cycle dysfunction and altered brain energy metabolism on modulation of glutamate receptors and transporters in acute and chronic hyperammonemia. Biomed. Pharmacother. 81, 192–202.

Nettesheim, S., Kolker, S., Karall, D., Haberle, J., Posset, R., Hoffmann, G.F., et al., 2017. Incidence, disease onset and short-term outcome in urea cycle disorders -cross-border surveillance in Germany, Austria and Switzerland. Orphanet J. Rare Dis. 12 (1), 111.

Ott, P., Vilstrup, H., 2014. Cerebral effects of ammonia in liver disease: current hypotheses. Metab. Brain Dis. 29 (4), 901–911.

Ott, P., Clemmesen, O., Larsen, F.S., 2005. Cerebral metabolic disturbances in the brain during acute liver failure: from hyperammonemia to energy failure and proteolysis. Neurochem. Int. 47 (1–2), 13–18.

Rao, K.V., Mawal, Y.R., Qureshi, I.A., 1997. Progressive decrease of cerebral cytochrome C oxidase activity in sparse-fur mice: role of acetyl-L-carnitine in restoring the ammonia-induced cerebral energy depletion. Neurosci. Lett. 224 (2), 83–86.

Ratnakumari, L., Qureshi, I.A., Butterworth, R.F., 1992. Effects of congenital hyperammonemia on the cerebral and hepatic levels of the intermediates of energy metabolism in spf mice. Biochem. Biophys. Res. Commun. 184 (2), 746–751.

Ratnakumari, L., Qureshi, I.A., Butterworth, R.F., Marescau, B., De Deyn, P.P., 1996. Arginine-related guanidino compounds and nitric oxide synthase in the brain of ornithine transcarbamylase deficient spf mutant mouse: effect of metabolic arginine deficiency. Neurosci. Lett. 215 (3), 153–156.

Salerno, F., Abbiati, R., Fici, F., 1983. Effect of pyridoxine alpha-ketoglutarate (PAK) on ammonia and pyruvic and lactic acid blood levels in patients with cirrhosis. Int. J. Clin. Pharmacol. Res. 3 (1), 21–25.

Sauer, S.W., Opp, S., Komatsuzaki, S., Blank, A.E., Mittelbronn, M., Burgard, P., et al., 2015. Multifactorial modulation of susceptibility to l-lysine in an animal model of glutaric aciduria type I. Biochim. Biophys. Acta 1852 (5), 768–777.

Shen, J., Petersen, K.F., Behar, K.L., Brown, P., Nixon, T.W., Mason, G.F., et al., 1999. Determination of the rate of the glutamate/glutamine cycle in the human brain by in vivo 13C NMR. Proc. Natl. Acad. Sci. U. S. A. 96 (14), 8235–8240.

Sibson, N.R., Mason, G.F., Shen, J., Cline, G.W., Herskovits, A.Z., Wall, J.E., et al., 2001. In vivo (13)C NMR measurement of neurotransmitter glutamate cycling, anaplerosis and TCA cycle flux in rat brain during. J. Neurochem. 76 (4), 975–989.

Slocum, R.H., Cummings, J.G., 1991. Amino acid analysis of physiological samples. In: Hommes, F.A. (Ed.), Techniques in Diagnostic Human Biochemical Genetics: A Laboratory Manual. Wiley-Liss, New York, pp. 87–126.

Steinke, D., Salzburger, W., Braasch, I., Meyer, A., 2006. Many genes in fish have species-specific asymmetric rates of molecular evolution. BMC Genomics 7, 20.

Strauss, G.I., Knudsen, G.M., Kondrup, J., Moller, K., Larsen, F.S., 2001. Cerebral metabolism of ammonia and amino acids in patients with fulminant hepatic failure. Gastroenterology 121 (5), 1109–1119.

Summar, M.L., Dobbelaere, D., Brusilow, S., Lee, B., 2008. Diagnosis, symptoms, frequency and mortality of 260 patients with urea cycle disorders from a 21-year, multicentre study of acute hyperammonaemic episodes. Acta Paediatr. 97 (10), 1420–1425.

Summar, M.L., Koelker, S., Freedenberg, D., Le Mons, C., Haberle, J., Lee, H.S., et al., 2013. The incidence of urea cycle disorders. Mol. Genet. Metab. 110 (1–2), 179–180.

Sweetman, L., 1991. Organic acid analysis. In: Hommes, F.A. (Ed.), Techniques in Diagnostic Human Biochemical Genetics: A Laboratory Manual. Wiley-Liss, New York, pp. 143–176.

Tofteng, F., Jorgensen, L., Hansen, B.A., Ott, P., Kondrup, J., Larsen, F.S., 2002. Cerebral microdialysis in patients with fulminant hepatic failure. Hepatology 36 (6), 1333–1340.

Tonjes, M., Barbus, S., Park, Y.J., Wang, W., Schlotter, M., Lindroth, A.M., et al., 2013. BCAT1 promotes cell proliferation through amino acid catabolism in gliomas carrying wild-type IDH1. Nat. Med. 19 (7), 901–908.

Tuchman, M., Lee, B., Lichter-Konecki, U., Summar, M.L., Yudkoff, M., Cederbaum, S.D., et al., 2008. Cross-sectional multicenter study of patients with urea cycle disorders in the United States. Mol. Genet. Metab. 94 (4), 397–402.

van Karnebeek, C.D., Sly, W.S., Ross, C.J., Salvarinova, R., Yaplito-Lee, J., Santra, S., et al., 2014. Mitochondrial carbonic anhydrase VA deficiency resulting from CA5A

alterations presents with hyperammonemia in early childhood. Am. J. Hum. Genet. 94 (3), 453–461.
Velvizhi, S., Dakshayani, K.B., Subramanian, P., 2002. Effects of alpha-ketoglutarate on antioxidants and lipid peroxidation products in rats treated with ammonium acetate. Nutrition 18 (9), 747–750.
Walsh, T.S., McLellan, S., Mackenzie, S.J., Lee, A., 1999. Hyperlactatemia and pulmonary lactate production in patients with fulminant hepatic failure. Chest 116 (2), 471–476.
Wang, Q., Wang, Y., Yu, Z., Li, D., Jia, B., Li, J., et al., 2014. Ammonia-induced energy disorders interfere with bilirubin metabolism in hepatocytes. Arch. Biochem. Biophys. 555 (556), 16–22.
Wendon, J.A., Harrison, P.M., Keays, R., Williams, R., 1994. Cerebral blood flow and metabolism in fulminant liver failure. Hepatology 19 (6), 1407–1413.
Yang, R.Z., Blaileanu, G., Hansen, B.C., Shuldiner, A.R., Gong, D.W., 2002. cDNA cloning, genomic structure, chromosomal mapping, and functional expression of a novel human alanine aminotransferase. Genomics 79 (3), 445–450.
Zielonka, M., Breuer, M., Okun, J.G., Carl, M., Hoffmann, G.F., Kolker, S., 2018. Pharmacologic rescue of hyperammonemia-induced toxicity in zebrafish by inhibition of ornithine aminotransferase. PLoS One 13 (9), e0203707.
Zwingmann, C., Chatauret, N., Leibfritz, D., Butterworth, R.F., 2003. Selective increase of brain lactate synthesis in experimental acute liver failure: results of a [H-C] nuclear magnetic resonance study. Hepatology 37 (2), 420–428.